Alloy Choice by Assessing Epistemic and Aleatory Uncertainty in the Crack Growth Rates

K. S. Bhachu[1], R. T. Haftka[2], N. H. Kim[3]
University of Florida, Gainesville, Florida, USA

and

C. Hurst[4]
Cessna Aircraft Company, Wichita, Kansas, USA

Abstract

In probabilistic damage tolerance design, the choice of aluminum alloy may be influenced by the uncertainty/scatter in the crack growth rate and corresponding failure life. The epistemic uncertainty (due to limited test data) in the crack growth model parameters may play a major role in the decision making along with the aleatory uncertainty (due to material variability). In this study, we estimate the epistemic uncertainty (via bootstrapping) and the aleatory uncertainty in the crack growth model parameters for 7475-T7351 and 7050-T7451 aluminum alloys. The choice between the alloys is made by comparing the reliability index estimated from respective crack growth failure life distributions. Finally, weight savings due to superior crack growth failure life of one alloy than other is estimated.

Introduction

The design of aircraft structures using probabilistic damage tolerance analysis (PDTA) involves modeling and propagation of uncertainties in the crack growth model inputs e.g. uncertainty in crack growth rate (i.e. da/dN vs. ΔK). We rely on experiments to estimate the best fit parameters of a crack growth model (e.g. Paris law, Walker equation). To estimate the uncertainty in fatigue crack growth life/failure life, these best fit parameters are treated as random variables and are the major source of aleatory uncertainty (due to material variability) and epistemic uncertainty (due to limited test data). Selection of aluminum alloy for a particular damage tolerance application (e.g. wing spar) is typically based on the compromise between various material properties, such as fracture toughness, crack growth rate, yield strength, and stress corrosion cracking behavior. Of all these, the crack growth rate plays an important role in designing a light weight structure. A designer needs to choose an alloy that would satisfy a given probability of failure/risk constraint (e.g. 10^{-4}) with minimum weight penalty. The choice could possibly depend on the uncertainty (amount of scatter) present in the crack growth rate/model parameters and corresponding failure life. Therefore, it is important to quantify and compare the uncertainty (i.e. total uncertainty by combining aleatory and epistemic uncertainties) in the crack growth life for various aluminum alloys. In this study, we compare the uncertainty in crack growth life for the two most common aerospace aluminum alloys i.e. 7475-T7351 and 7050-T7451 plate materials. We compare both alloys under constant amplitude loading spectrum.

The comparison is based on comparing the reliability indices (β's) that are estimated from the crack growth failure life distribution for nominally identical specimen geometry. Then, weight savings due to better crack growth rate behavior is estimated i.e. an alloy with superior (larger) failure life will satisfy a given probability of failure constraint with lesser cross-sectional area, resulting in weight savings over other alloy.

Test Data and Crack Growth Model

Crack Growth Test Data

The crack growth rate data (da/dN vs. ΔK) is derived from the crack length (a) vs. load cycle (N) data. The a vs. N data is obtained by laboratory testing of crack test specimens e.g. middle tension M(T) crack test specimen shown

[1] Doctoral Student, Dept. of Mechanical & Aerospace Engineering, kdsbhachu@gmail.com, AIAA Student Member.
[2] Distinguished Professor, Dept. of Mechanical & Aerospace Engineering, haftka@ufl.edu, AIAA Fellow.
[3] Associate Professor, Dept. of Mechanical & Aerospace Engineering, nkim@ufl.edu, AIAA associate Fellow.
[4] Sr. Specialist Engineer, Fatigue & Damage Tolerance Dept., churst@cessna.textron.com.

in Figure 1. A symmetric double through crack of total length (2*c*) is grown from a small hole of diameter (*d*) centered in a rectangular aluminum plate of width (W) and thickness (B). These tests are typically performed under constant amplitude loading ($\Delta P = P_{max} - P_{min}$ = constant) that are then used to predict the crack growth life under variable amplitude loading. In order to capture the stress ratio (R)/mean stress effects, tests are repeated at specific stress ratios (e.g. at R = 0.05, 0.3, 0.5, and 0.7). The stress ratio (*R*) is defined by the following relationship,

$$R = \frac{S_{\min}}{S_{\max}} = \frac{P_{\min}}{P_{\max}} \quad . \tag{1}$$

Where, S_{min} and P_{min} are the minimum stress and load for a given load cycle; S_{max} and P_{max} are the maximum stress and load occurring in a given load cycle.

The crack growth rate (*da*/*dN*) is defined as the rate of crack extension with number of applied load cycles. The slope of *a* vs. *N* data is converted into *da*/*dN* vs. Δ*K* data by various data reduction techniques. We have used ASTM's quadratic 7-point incremental polynomial method [1] for deriving crack growth rate data. A sample *a* vs. *N* data for 7475-T7351 alloy for 25 specimens tested under four different stress ratios is shown in Figure 2, and corresponding *da*/*dN* vs. Δ*K* data is shown in Figure 3.

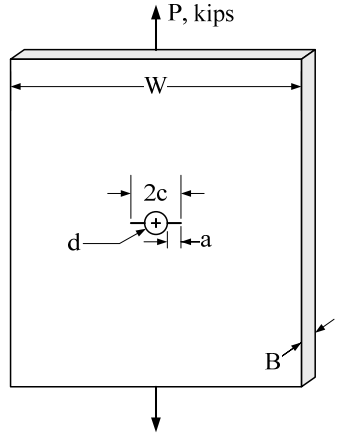

Fig. 1 Middle tension M(T) crack specimen.

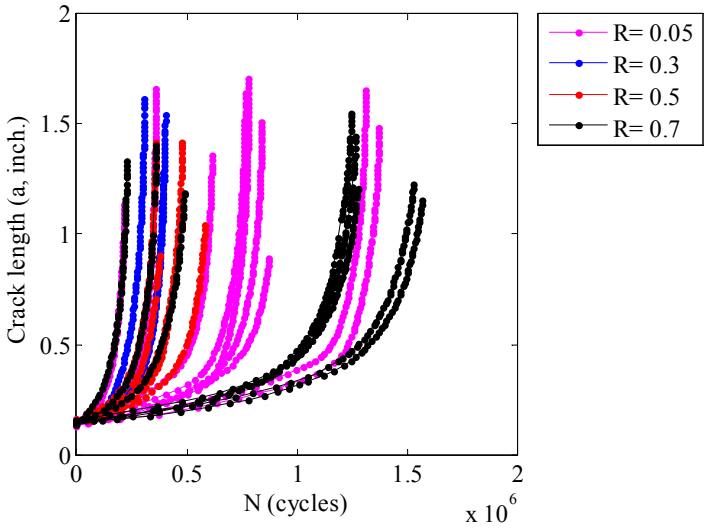

Fig. 2 Crack length (a) vs. load cycles (N) data for 7475-T7351 alloy.

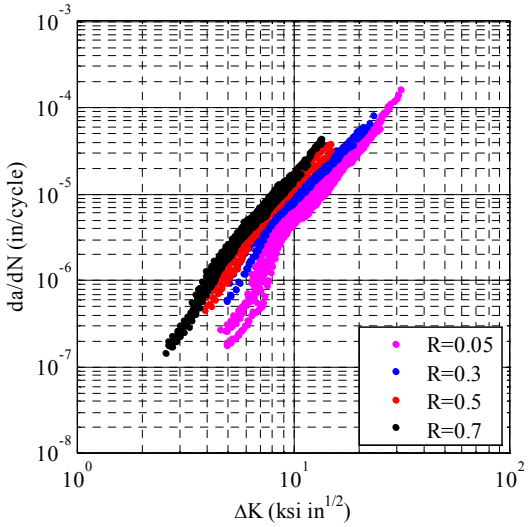

Fig. 3 Crack growth rate data for 7475-T7351 alloy.

Crack Growth Model

The crack growth life for design applications is predicted by fitting a crack growth model to the laboratory test data. Detailed fitting procedure is discussed in the next section. The scatter/uncertainty in failure lives is usually estimated via Monte Carlo Simulation [2-5]. This first requires the estimation of uncertainty in the crack growth model parameters e.g. estimation of the statistical distributions of C and n if Paris law is used,

$$\frac{da}{dN} = C\left(\Delta K\right)^n . \tag{2}$$

Where, da/dN is the crack growth rate; ΔK is the stress intensity; C is Paris constant; and n is Paris exponent. The crack tip stress intensity is the function of loading/stress range (ΔS) and specimen geometry,

$$\Delta K = G_{CF}\Delta S\sqrt{\pi a} . \tag{3}$$

The stress range (remote stress) is related to applied load and geometry by the following relationship,

$$\Delta S = \frac{\Delta P}{\left(BW\right)} = \frac{P_{\max} - P_{\min}}{\left(BW\right)} . \tag{4}$$

Half crack length a (inch.) is related to the specimen geometry as follows,

$$a = \frac{1}{2}\left(2c - d\right) = c - r . \tag{5}$$

The geometric correction factor G_{CF} is a function of infinite plate solution $G_{CF\infty}$ and finite width correction factor F_{WC},

$$G_{CF} = G_{CF\infty}F_{WC} , \tag{6}$$

$$G_{CF\infty} = \sqrt{\sec\left(\frac{\pi r}{W}\right)\sec\left(\frac{\pi\left(a+r\right)}{W}\right)} , \tag{7}$$

$$F_{WC} = 1.0014 + 0.4818\left(\frac{r}{a+r}\right) + 0.2406\left(\frac{r}{a+r}\right)^2 + 0.684\left(\frac{r}{a+r}\right)^3 + 0.9561\left(\frac{r}{a+r}\right)^4 . \tag{8}$$

A reliable estimation of the distributions of the crack model parameters requires sufficient test data at a given test condition i.e. combination of (ΔS) and stress ratios (R). In the absence of sufficient data for a particular test condition, estimation of the distributions of crack model parameters can be aided by pooling data from other combinations of test conditions [4].

Crack Growth Model

We have used walker equation for modeling the crack growth rate and predicting the failure lives. The usefulness of walker model is due to its ability to account for stress ratio effects [6] while retaining the simplicity of the Paris law.

$$\widehat{\frac{da}{dN}} = C\left[\Delta K\left(1-R\right)^{m-1}\right]^{n} \tag{9}$$

Where, m is the walker constant that varies between 0 and 1. A value of m closer to 0 shows strong stress ratio effect, and for m=1 the above equation reduces to the Paris law i.e. no stress ratio effect.

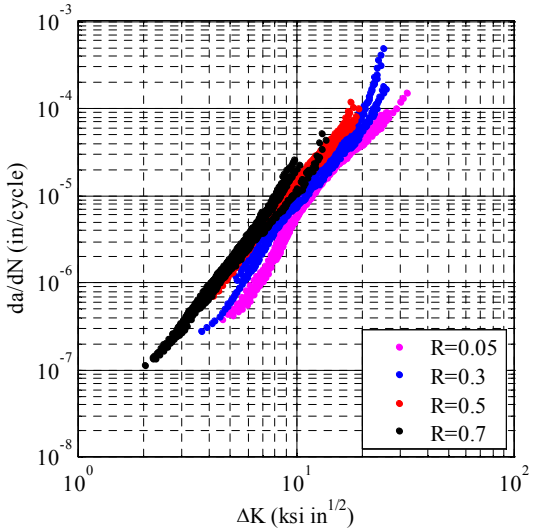

Fig. 4 Original crack growth data for 7050-T7451

Walker Equation Fitting

In practice, a segmented (multi-slope) walker equation is used to fit the crack growth rate data [], which is useful for the purpose of more accurate life prediction. But, for the purpose of comparing different alloys, a single slope walker equation would be sufficient. A closer look at the Figure 5 shows that differences between alloys can be expected when cracks are small or when crack growth rate values are small (i.e. when $da/dN < 10^{-6}$ in./cycle).

A crack usually spends significant portion of its life growing in smaller da/dN vs. ΔK region, so it is important to capture the variability in growth rate more accurately for this region. With single slope fit, if sum of error squares in da/dN is minimized, then fit is naturally more accurate for higher da/dN vs. ΔK region. But, fit can be made more accurate for lower da/dN vs. ΔK region by simply minimizing the sum of error square in the inverse da/dN (i.e. dN/da). The L-2 norm of the errors in inverse crack growth rate prediction is given as follows,

$$\left\|\varepsilon\right\|_2^2 = \sum_{i=1,j=1,k=1}^{n_s,n_R,n_p}\left[1\Big/\left(\frac{da}{dN}\right)_{ijk} - 1\Big/\left(\widehat{\frac{da}{dN}}\right)_{ijk}\right]^2. \tag{10}$$

Where, n_s is number of specimens; n_R is number of different stress ratios; and n_p is the number of data points for i^{th} specimen with j^{th} stress ratio.

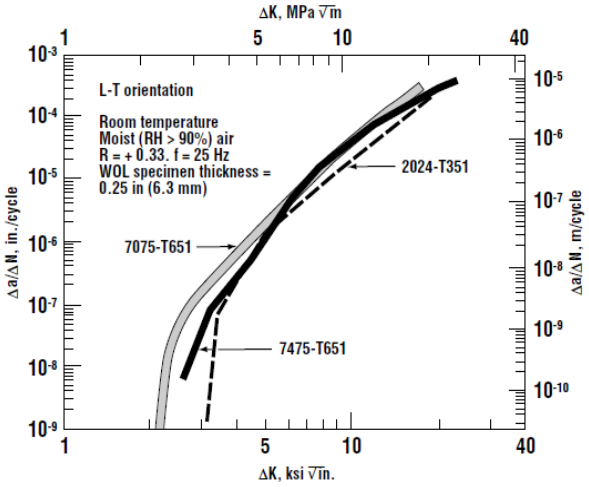

Fig. 5 Crack growth rate comparison between alloys [8].

The walker equation is nonlinear in parameters. So, the minimization of L-2 norm is an iterative process, which requires an optimization procedure to find the best fit parameters. The minimization is carried out by using '*fminsearch*' function available in the optimization toolbox of the MATLAB. The best fit walker parameters (listed in Table) consolidates/collapses the original test data (shown in Figures) onto the best fit walker line (for R =0) is shown in Figure 6 for 7475-T7351 and Figure 7 for 7050-T7451.

Table 1 Best fit Walker parameters

Alloy	C*	n*	m*
7475-T7351	2.526×10^{-10}	4.240	0.534
7050-T7451	2.458×10^{-09}	3.254	0.647

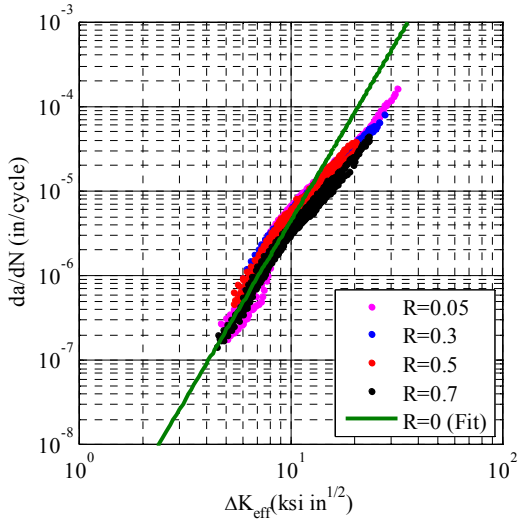

Fig. 6 Collapsed crack growth data and Walker fit for 7475-T7351 alloy.

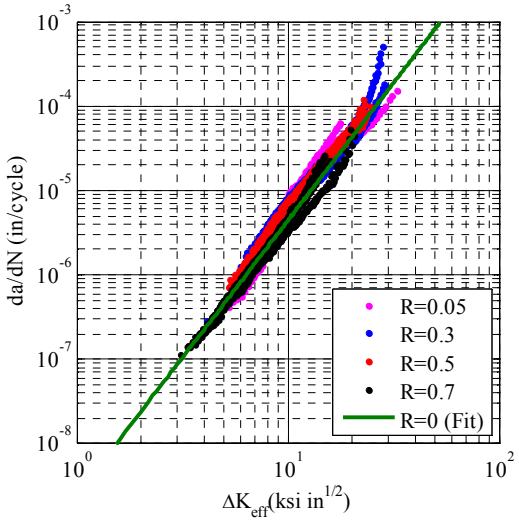

Fig. 7 Collapsed crack growth data and Walker fit for 7050-T7451 alloy.

Uncertainty Sources

The most common classification of uncertainty in the risk analysis community categorizes it into aleatory and epistemic uncertainty [9].

1. Aleatory Uncertainty
   Aleatory uncertainty is due to inherent variations or randomness, which in this case is due to variability in the crack growth rate. Aleatory uncertainty is also sometimes referred as irreducible uncertainty, in the context that it cannot be reduced by collecting more test data. While, aleatory uncertainty can be reduced by improving the quality control. This type of uncertainty is generally characterized by the probability distributions that are estimated by fitting various continuous parametric distributions to the data. However, we have directly used the discrete sample set (i.e. test data) to model the aleatory uncertainty.

2. Epistemic Uncertainty
   Epistemic uncertainty is due to the lack of knowledge, which in this case is due to the limited amount of test data e.g. 25 test samples for 7475-T7351 alloy. The best fit parameters of the walker equation are estimated from only 25 samples, but the true value (i.e. population based estimate) of the best fit parameters would be any possible value about the sample based estimate of the best fit parameters. Therefore, this kind of uncertainty can be reduced by collecting more test data. We have estimated the epistemic uncertainty via non-parametric bootstrapping. It allows us to estimate the sampling distribution (representing epistemic uncertainty) of the best fit parameters without making assumptions about the form of the population. The procedure is discussed in detail in the next section.

Uncertainty Propagation

The aleatory and epistemic uncertainty in the walker equation parameters is propagated by Monte Carlo simulation. It is a double loop process, where epistemic sample is first generated via non-parametric bootstrapping. Then aleatory uncertainty is estimated for each epistemic sample, which gives the total uncertainty in the best fit parameters and corresponding failure life.

Epistemic Uncertainty Estimation via Bootstrapping

The epistemic uncertainty is estimated via bootstrapping i.e. resampling (with replacement) the specimens tested for different stress ratios (R), and fitting walker equation to each bootstrap sample. The detailed procedure is shown in Figure 8, where first step is to estimate the best fit walker parameters (i.e. C*, n*, m*) by using the original test data. Then bootstrap samples are generated by resampling the test specimens from the original sample. The walker equation is then refitted to each bootstrap sample, where walker constant 'm' is fixed for each bootstrap sample, and is fixed to the best fit value (i.e. m*) that was estimated from the original sample. The only purpose of walker constant is to collapse data onto single line (as shown in Figures 6-7). The bootstrapping is repeated a million times, which gives sampling distribution of the best fit parameters. The sampling distribution of 'C' and 'n' for both

alloys (7475-T7351 and 7050-T7451) representing epistemic uncertainty in the parameters is shown in Figures 8-11. The statistics of sampling distributions are listed in Table 2, where coefficient of variation (COV) for 7475-T7351 (22.6% for *C*, and 3.08% for *n*) is higher than for 7050-T7451 (7.34% for *C*, and 1.4% for *n*), partly due to difference in the number of samples available for fitting i.e. 25 vs. 30 samples, and partly due to more repeatable data available for 7050-T7451.

Table 2 Statistics of sampling distributions of walker model parameters

Alloy	Paris constant (C)			Paris exponent (n)			Correlation
	μ	σ	COV	μ	σ	COV	ρ
7050-T7451	2.4393×10^{-9}	1.7897×10^{-10}	7.34%	3.260	0.048	1.4%	-0.980
7475-T7351	2.5361×10^{-10}	5.7340×10^{-11}	22.6%	4.253	0.131	3.08%	-0.964

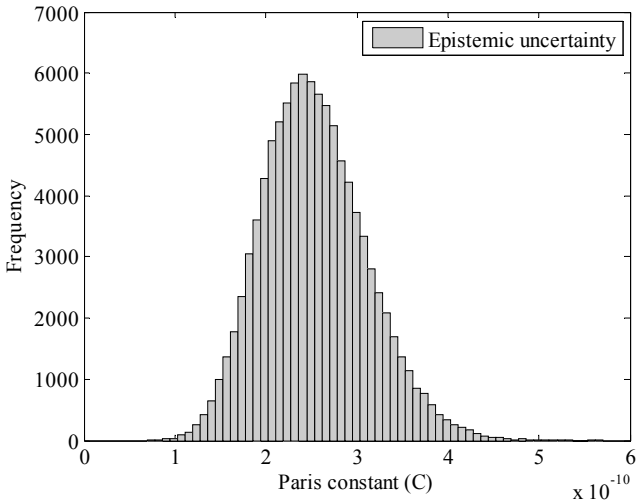

Fig. 8 Sampling distribution of *C* for 7475-T7351 alloy.

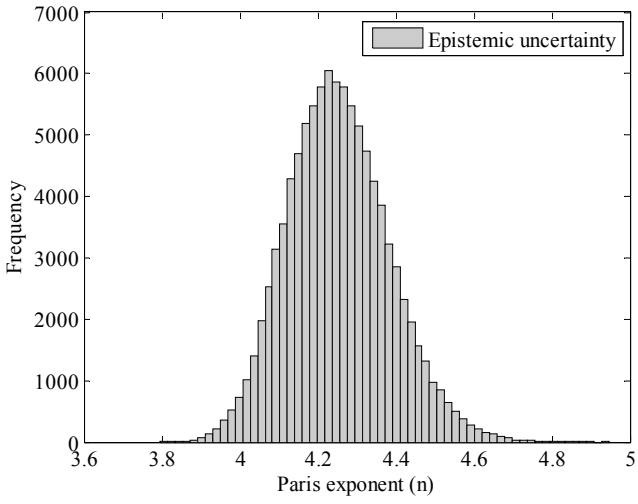

Fig. 9 Sampling distribution of *n* for 7475-T7351 alloy.

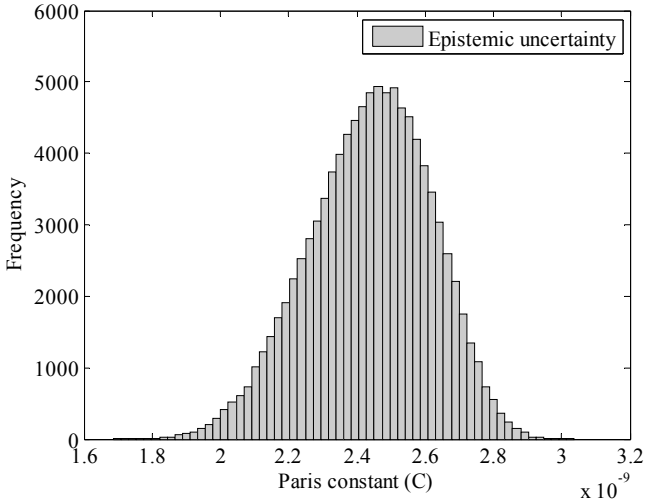

Fig. 10 Sampling distribution of *C* for 7050-T7451 alloy.

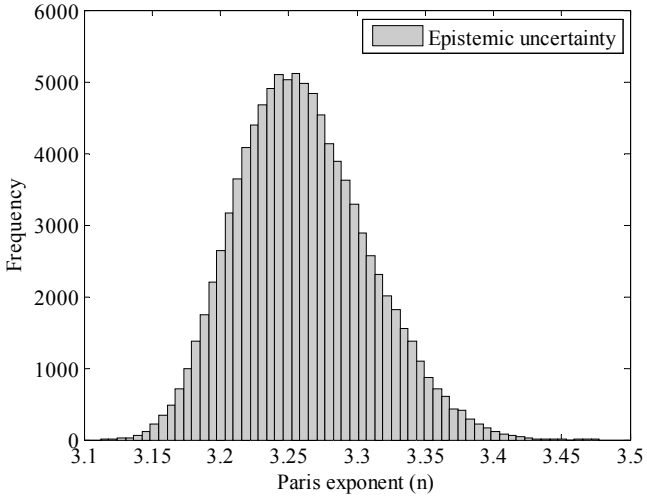

Fig. 11 Sampling distribution of *n* for 7075-T7451 alloy.

Aleatory Uncertainty Estimation

The aleatory uncertainty in the best fit walker equation parameter (C) is estimated by fixing the Paris exponent n (m is already fixed to m^*), where n is drawn (i.e. epistemic sample) from the sampling distribution determined earlier. The walker equation is then fitted separately to the data from each individual test specimen in the original sample [5]. For example in Figure 14, if we consider the best fit parameters for the original sample as one instance of the epistemic uncertainty/bootstrap sample, then while estimating the aleatory uncertainty (by refitting each individual test specimen data separately with the walker equation) n and m will be fixed to n^* and m^*, with only variable allowed to change being C. This gives one possible realization (i.e. distribution) of the aleatory uncertainty in C. The aleatory uncertainty in C estimated for the original sample is shown in Figure 12 for 7475-T7351 (COV = 25.7%) and in Figure 13 for 7050-T7451 (COV = 28.6%). Related statistics are shown in Table 3.

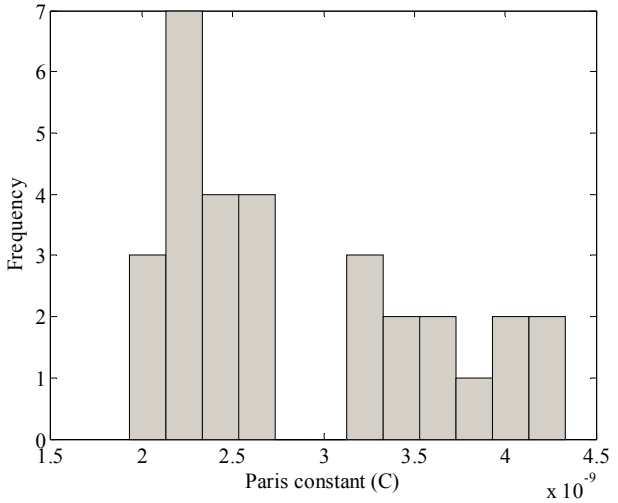

Fig. 12 Aleatory uncertainty in C for 7050-T7451 alloy (30 samples)

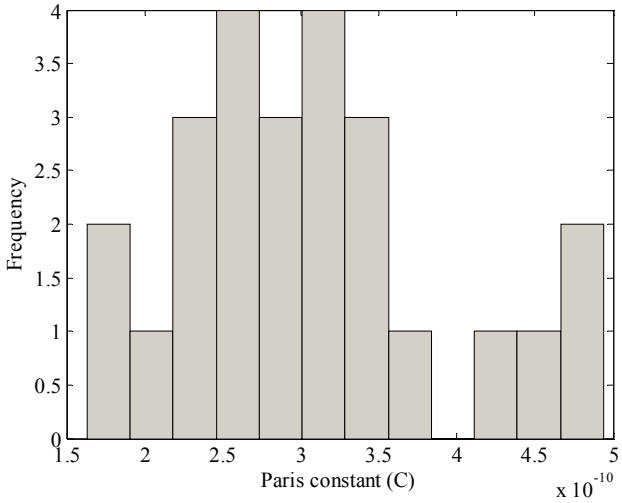

Fig. 13 Aleatory uncertainty in C for 7475-T7351 alloy (25 samples)

Table 3 Statistics of aleatory distribution of walker model parameters

Alloy	Paris constant (C)			Paris constant (n)	Walker constant (m)
	μ	σ	COV		
7050-T7451	2.8509×10^{-9}	7.3360×10^{-10}	25.7%	4.240	0.534
7475-T7351	3.0722×10^{-10}	8.6605×10^{-11}	28.6%	3.254	0.647

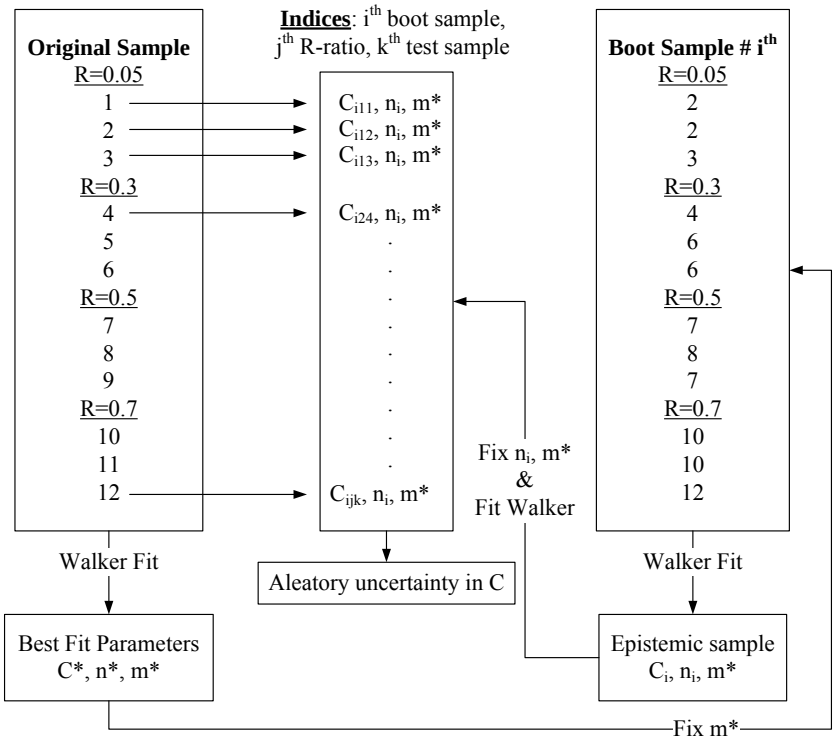

Fig. 14 Epistemic and aleatory uncertainty propagation

Total uncertainty

Estimating the aleatory uncertainty in parameter *C* by using the procedure shown in Figure 14 for every bootstrap sample (with *n* fixed to best fit estimate n_i of that particular bootstrap sample) gives us the total uncertainty in parameter *C*. The total uncertainty in *C* for 7475-T7351 and 7050-T7451 is shown in Figures 15-16. Associated statistics are listed in Table 4.

Table 4 Total uncertainty statistics for Paris constant *C*.

Alloy	Paris constant (C)		
	μ	σ	COV
7050-T7451	2.8283×10^{-9}	7.5725×10^{-10}	26.8%
7475-T7351	3.0827×10^{-10}	1.1367×10^{-10}	36.9%

Bi-modal shape of the distribution shown in Figure is due to the uneven aleatory distribution of the original data set (i.e. notice large gap in Figure 12). For different values of *n* (i.e. epistemic samples from bootstrapping), the distribution of *C* keeps on building around the original distribution, such that big gap does not get filled up. Such phenomenon is not seen for 7475-T7351 due to more evenly spaced aleatory distribution i.e. very small gaps in the histogram of *C* as shown in Figure 13.

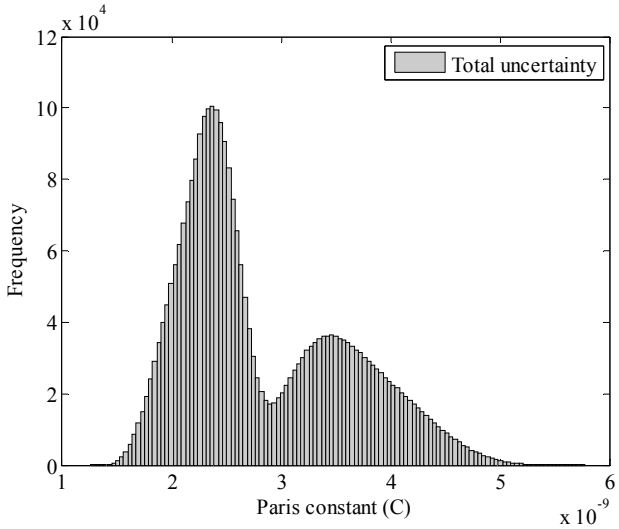

Fig. 15 Total uncertainty in *C* for 7050-T7451 alloy.

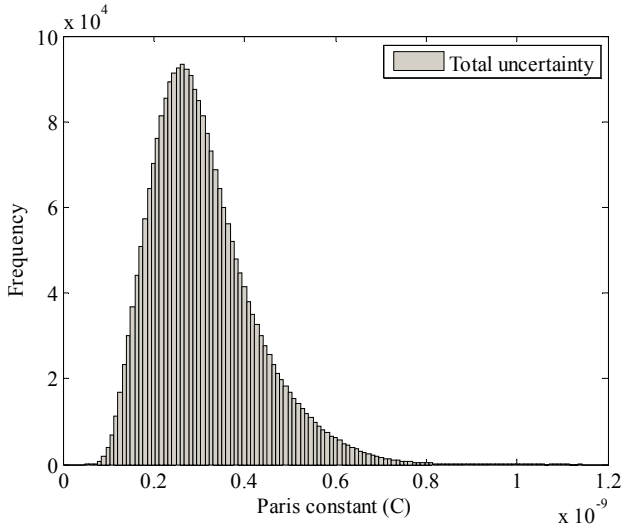

Fig. 16 Total uncertainty in *C* for 7475-T7351 alloy

Test Geometry and Stress Spectrum for Simulation

The total uncertainty in best fit model parameters (C and n) found in the previous section need to be converted into uncertainty in the crack growth life/failure life. In order to compare the two alloys, a reliability index will be calculated using the failure life distributions. These distributions will be determined for nominally identical specimen geometry, and load spectrum.

In practice, the reliability based design procedure requires a given risk/probability of failure (P_f) constraint to be satisfied on the failure life (e.g. $P_f \leq 10^{-7}$), where failure life (N_f) is at least equal to the design service goal (N_{dsg}); i.e., $N_f \geq N_{dsg}$. N_{dsg} of 24,000 flight hours (FH) is a typical design service goal for a mid-size business jet. Basically, structural sizing is done to meet the design service goal while maintaining certain acceptable probability of failure. In this case, $P_f \leq 10^{-4}$ is thought to be adequate due to the conservative assumptions made for the other inputs e.g. rogue flaw size (a_{rf}) of 0.05".

Test Geometry

The specimen geometry used for comparing the failure life distributions of the two alloys has the same configuration as that of the middle tension M(T) crack specimen shown in Figure 1. The width (W) of the specimen is fixed at 4" because 7475-T7351 alloy plate material is not available in thickness greater than 4", and diameter of the hole is d= 0.05". The thickness (B) of the test geometry is a free variable that is found such that 0.01 percentile

failure life ($N_{f0.01\%}$) should be greater than 24,000 flight hours (FH). The $N_{f0.01\%}$ translates into the probability of failure (P_f) constraint of 10^{-4}.

Constant Amplitude Stress Spectrum

The constant amplitude load spectrum is used for executing the crack growth analyses. It allows using the integral form of the walker equation to estimate the failure life instead of using a cycle-by-cycle integration scheme,

$$N = \frac{1}{C\left[\Delta S\left(1-R\right)^{1-m}\right]^{n}} \int_{a_{rf}}^{a_f} \left(G_{CF}\sqrt{\pi a}\right)^{-n} da \,. \tag{11}$$

Where, a_{rf} is a rogue flaw of length 0.05", and a_f is a failure causing crack length estimated by K_{max} failure criterion i.e. $K_{max} \geq K_{IC}$ (K_{IC} is plane strain fracture toughness). The integrand in the above equation is solved by the numerical integration. A comparison between the alloys is made for two different loading conditions shown in Table 5.

Table 5 Test conditions defining constant amplitude load spectrum

Test condition	Max. load (P_{max}, kips)	Stress Ratio (R)
1	3.456	0.05
2	7.290	0.7

Failure Life Distribution, Reliability Index, and Weight Savings

The failure distributions for both alloys using nominally identical geometry and test condition 1 are shown in Figures 17-18, and corresponding statistics are listed in Table 6.

The distribution of 7050-T7451 turns out to be bi-modal due to bi-modal shape of parameter C distribution as shown in Figure. Notice that 0.01 percentile failure life ($N_{f0.01\%}$) satisfies the requirement of being above design service goal of 24,000 FH for both the alloys. The coefficient of variation (COV) for 7475 (35.8%) is higher than that of 7050 (24.1%) indicating more scatter in the 7475 data. The mean failure life (μ_{Nf}) of 7475 is about 6.9 times higher than of 7050 for the nominally identical geometry. Also, uncertainty/standard deviation for 7475 is about 10.2 times higher than that of 7050. The reliability index (β) is calculated by using the following equation,

$$\beta = \frac{\mu_{Nf} - N_{dsg}}{\sigma_{Nf}} \,. \tag{12}$$

The reliability index of 7475-T7351 is greater than that of 7050-T7351, which indicates the usefulness (through weight savings) of choosing 7475-T7351 for probabilistic damage tolerant design. Similar trend is seen for the test condition 2; the statistics are shown in Table 7.

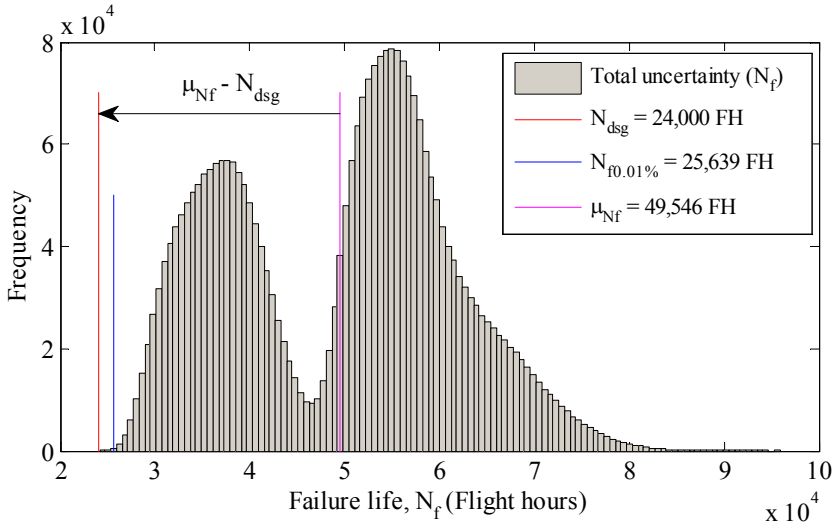

Fig. 17 Failure life distribution for 7050-T7451 alloy

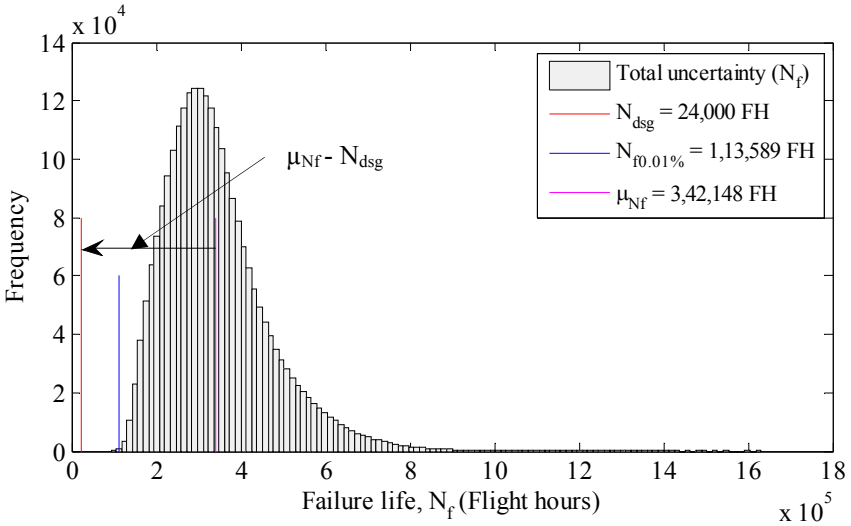

Fig. 18 Failure life distribution for 7475-T7351alloy

Table 6 Failure life distribution statistics for test condition 1

Alloy	Failure life (N_f, flight hours)			Reliability index
	μ	σ	COV	ρ
7050-T7451	49,546	11,950	24.1%	2.14
7475-T7351	3, 42,148	1, 22,308	35.8%	2.60

Table 7 Failure life distribution statistics for test condition 2

Alloy	Failure life (N_f, flight hours)			Reliability index
	μ	σ	COV	ρ
7050-T7451	49,356	11,904	24.1%	2.13
7475-T7351	1,95,177	67,576	34.62%	2.53

Next logical step is to estimate the weight savings if 7475-T7351 is used in the design. The weight savings are achieved by decreasing the thickness of specimen (i.e. allowing for higher stress) while satisfying the failure life constraint ($N_{f0.01\%} \geq N_{dsg}$) as closely as possible. The thickness reduction of 0.128" (0.45"-0.322")/28% is estimated for test condition 1, and 0.9" (0.45"-0.36")/20% for the test condition 2 (see Table 8). Notice that the ratio of $N_{f0.01\%}/N_{dsg}$ is higher for 7475 (1.18) than 7050 (1.07), indicating that thickness could further be reduced. It will bring weight reduction estimates from both test conditions much closer.

Table 8 Statistics of failure distribution for 7475-T7351 alloy after thickness reduction, and weight savings

Test condition	Failure life (N_f, flight hours)				Reliability index	Initial thickness	Final thickness	Weight savings
	μ	σ	COV	$N_{f0.01\%}$	ρ	(B, inch.)	(B, inch.)	
1	74, 867	24, 638	33%	28, 290	2.06	0.45	0.322	28.4%
2	75, 180	24, 746	33%	28,399	2.06	0.45	0.360	20.0%

Concluding Remarks

The uncertainty/scatter in the failure life for 7475 was found to be higher than that of 7050-T7451 alloy. Instead of higher uncertainty, the reliability index of 7475-T7351 was higher than that of 7050-T7351, indicating higher mean life compensating for the higher uncertainty. It is concluded that for the data used in this study, 7475-T7351 will provide structure with lower weight than 7050-T7351 when probabilistic damage tolerant design methods are employed.

Future Work

We will repeat the procedure using variable amplitude load spectrum taken from the wing location of a business jet. Also, we will attempt to calculate B-basis values of fatigue crack growth life, which penalizes epistemic uncertainty more than the aleatory uncertainty.

Acknowledgement

We are thankful to NSF grant for the monetary support, and Cessna Aircraft Company for sharing the crack growth rate test data.

References

[1] "Standard Test Method for Measurement of Fatigue Crack Growth Rates", ASTM Standard E647-13ε1, 2013.

[2] Ostergaard, D. F. and Hillberry, B. M., "Characterization of the Variability in Fatigue Crack Propagation Data", Probabilistic Fracture Mechanics and Fatigue Methods: Applications for Structural Design and Maintenance, ASTM STP 798, 1983, pp. 97-115.

[3] Annis, C., "Probabilistic Life Prediction Isn't as Easy as It Looks", Probabilistic Aspects of Life Prediction, ASTM STP 1450, 2004, pp. 3-14.

[4] Johnston, G. O., "Statistical Scatter in Fracture Toughness and Fatigue Crack Growth Rate Data", Probabilistic Fracture Mechanics and Fatigue Methods: Applications for Structural Design and Maintenance, ASTM STP 798, 1983, pp. 42-66.

[5] Millwater, H. R., Weiland, D. H., "Probabilistic Sensitivity-Based Ranking of Damage Tolerance Analysis Elements", Journal of Aircraft, 2010, Vol. 47, No. 1, pp. 161-171.

[6] Walker, K., "The Effect of Stress Ratio During Crack Propagation and Fatigue for 2024-T3 and 7075-T6 Aluminum", Effect of Environment and Complex Load History on Fatigue Life, ASTM STP 462, 1970, pp.

[7] Hariharan, K., Prakash, R. V., "A Study of Multi-Segment Fatigue Crack Growth Analysis Procedure for Probabilistic Crack Growth Prediction", International Journal of Fatigue.

[8] Aloca Product Catalog, Retrieved from, http://www.alcoa.com/mill_products/catalog/pdf/alloy7075techsheet.pdf

[9] Roy, C. J., Oberkampf, W. L., "A Complete Framework for Verification, Validation, and Uncertainty Quantification in Scientific Computing", 48th AIAA Aerospace Sciences Meeting, 2010, Orlando, Florida.